Science Advances
AAAS

Supplementary Materials for

An estrogen-sensitive hypothalamus-midbrain neural circuit controls thermogenesis and physical activity

Hui Ye, Bing Feng, Chunmei Wang, Kenji Saito, Yongjie Yang, Lucas Ibrahimi, Sarah Schaul, Nirali Patel, Leslie Saenz, Pei Luo, Penghua Lai, Valeria Torres, Maya Kota, Devin Dixit, Xing Cai, Na Qu, Ilirjana Hyseni, Kaifan Yu, Yuwei Jiang, Qingchun Tong, Zheng Sun, Benjamin R. Arenkiel, Yanlin He*, Pingwen Xu*, Yong Xu*

*Corresponding author. Email: yongx@bcm.edu (Y.X.); pingwenx@uic.edu (P.X.); yanlin.he@pbrc.edu (Y.H.)

Published 19 January 2022, *Sci. Adv.* **8**, eabk0185 (2022)
DOI: 10.1126/sciadv.abk0185

This PDF file includes:

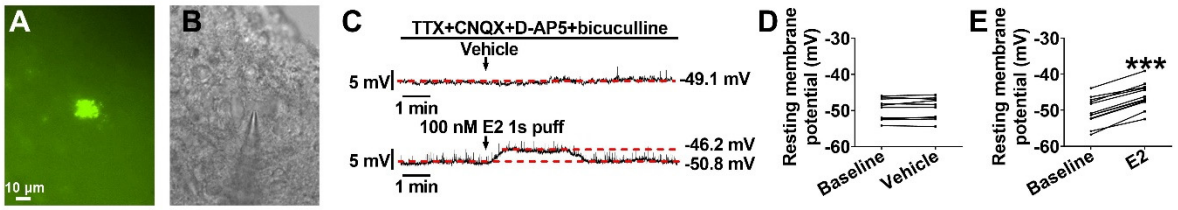

Figure S1 (Related to Figure 1). **E2 directly depolarizes ERα^{vlVMH} neurons**. **(A-B)** Micrographic images showing a recorded ERα-ZsGreen (+) neurons in the vlVMH of female mice. Left panel (A): the neuron visualized under the green fluorescence microscope; right panel (B): the same neuron patch clamped by a micropipette visualized under the brightfield microscope. Scale bar = 10 μm. **(C)** Representative resting membrane potential traces before and after vehicle or E2 treatment (100 nM, 1s puff) after pre-incubation of presynaptic inhibitors 1μM TTX (a voltage-gated sodium channel blocker) + 30μM CNQX (an AMPA receptor antagonist) + 30μM AP-5 (an NMDA receptor antagonist) + 50μM bicuculline (a $GABA_A$ receptor antagonist) in ZsGreen (+) cells. **(D-E)** Summary of resting membrane potential before and after vehicle (D) or E2 (E) treatment (n=10 or 12). (D-E) Data are presented for each cell. ***, $P < 0.001$ in paired t-tests.

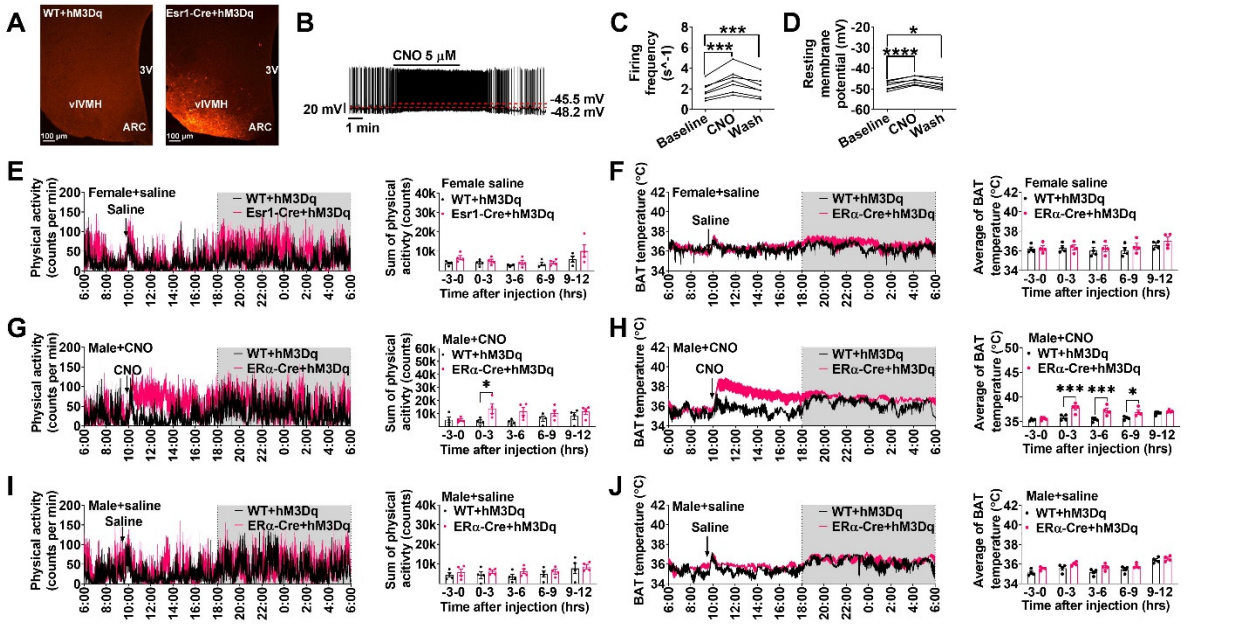

Figure S2 (Related to Figure 1). **Chemogenetic activation of ERα^{vlVMH} neurons stimulates physical activity and BAT thermogenesis in males**. **(A)** Immunofluorescence staining for mCherry in the vlVMH of WT + hM3Dq and Esr1-Cre + hM3Dq female mice. **(B)** Representative traces before and after CNO treatment (5 μM) from mCherry (+) cells in the vlVMH of Esr1-Cre + hM3Dq female mice. **(C-D)** Summary of firing frequency (C) and resting membrane potential (D) before and after CNO treatment (n =7). **(E)** Effects of saline i.p. injection on physical activity during 24-hrs recording (left panel) and sum of physical activity from 3 hours before to 12 hours after injection (right panel) in female WT + hM3Dq or Esr1-Cre + hM3Dq mice with emitter implanted under BAT (n =4 or 4). **(F)** Effects of saline injection on BAT temperature during 24-hrs recording (left panel) and average of BAT temperature from 3 hours before to 12 hours after injection (right panel) in female WT + hM3Dq or Esr1-Cre + hM3Dq mice (n = 4 or 4). **(G)** Effects of CNO injection on physical activity during 24-hrs recording (left panel) and sum of physical activity from 3 hours before to 12 hours after injection (right panel) in male WT + hM3Dq or Esr1-Cre + hM3Dq mice with emitter implanted under BAT (n = 4 or 4). **(H)** Effects of CNO injection on BAT temperature during 24-hrs recording (left panel) and average of BAT temperature from 3 hours before to 12 hours after injection (right panel) in male WT + hM3Dq or Esr1-Cre + hM3Dq mice (n = 4 or 4). **(I)** Effects of saline i.p. injection on physical activity during 24-hrs recording (left panel) and sum of physical activity from 3 hours before to 12 hours after injection (right panel) in male WT + hM3Dq or Esr1-Cre + hM3Dq mice with emitter implanted under BAT (n =4 or 4). **(J)** Effects of saline injection on BAT temperature during 24-hrs recording (left panel) and average of BAT temperature from 3 hours before to 12 hours after injection (right panel) in male WT + hM3Dq or Esr1-Cre + hM3Dq mice (n = 4 or 4). (C-D) Data are presented for each cell. **, $P < 0.01$, ***, $P < 0.001$ in repeated-measures ANOVA analysis followed by post hoc Dunnett tests. (E-J) Results are shown as mean ± SEM. *, $P < 0.05$ ***, $P < 0.001$ in two way ANOVA analysis followed by post hoc Sidak tests.

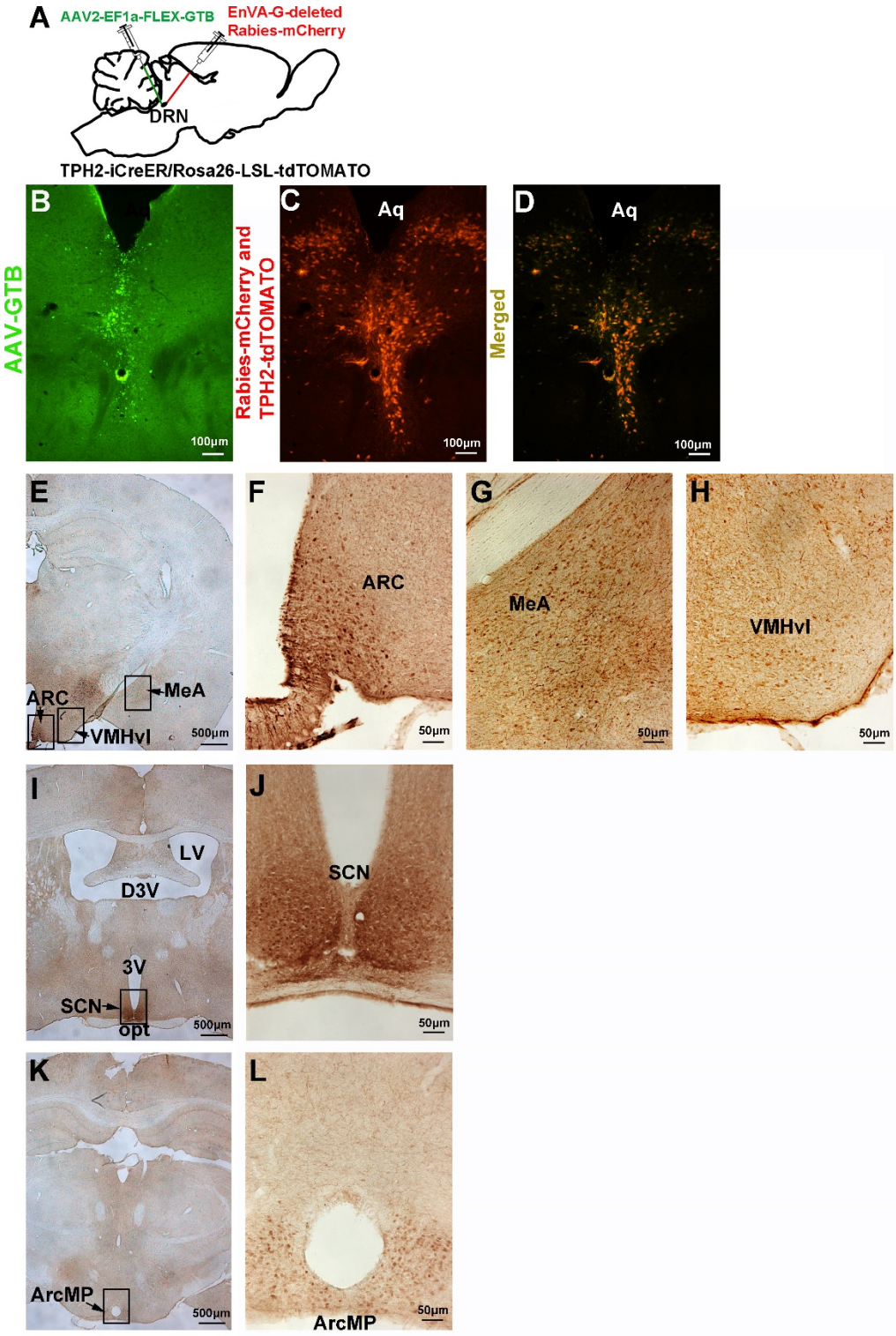

Figure S3 (Related to Figure 2). **Monosynaptic retrograde tracing from TPH2 neurons in the DRN**. **(A)** Schematic of the experimental strategy using the EnVA-G-deleted Rabies-mCherry virus as a monosynaptic tracer to identify the neuroanatomical inputs for $TPH2^{DRN}$ neurons. **(B-D)** Fluorescence of Enhanced green fluorescent protein + TVA + rabies B19 glycoprotein (GTB, green, B), mCherry (red, C),

and merger (D) in the DRN. **(E-L)** Immunoreactivity of mCherry (brown) in the arcuate nucleus of the hypothalamus (ARC, E and F), medial amygdala (MeA, E and G), vlVMH (E and H), suprachiasmatic nucleus (SCN, I and J), and medial posterior part of the Arc (ArcMP, K and L) of female TPH2-iCreER/Rosa26-LSL-tdTOMATO mice.

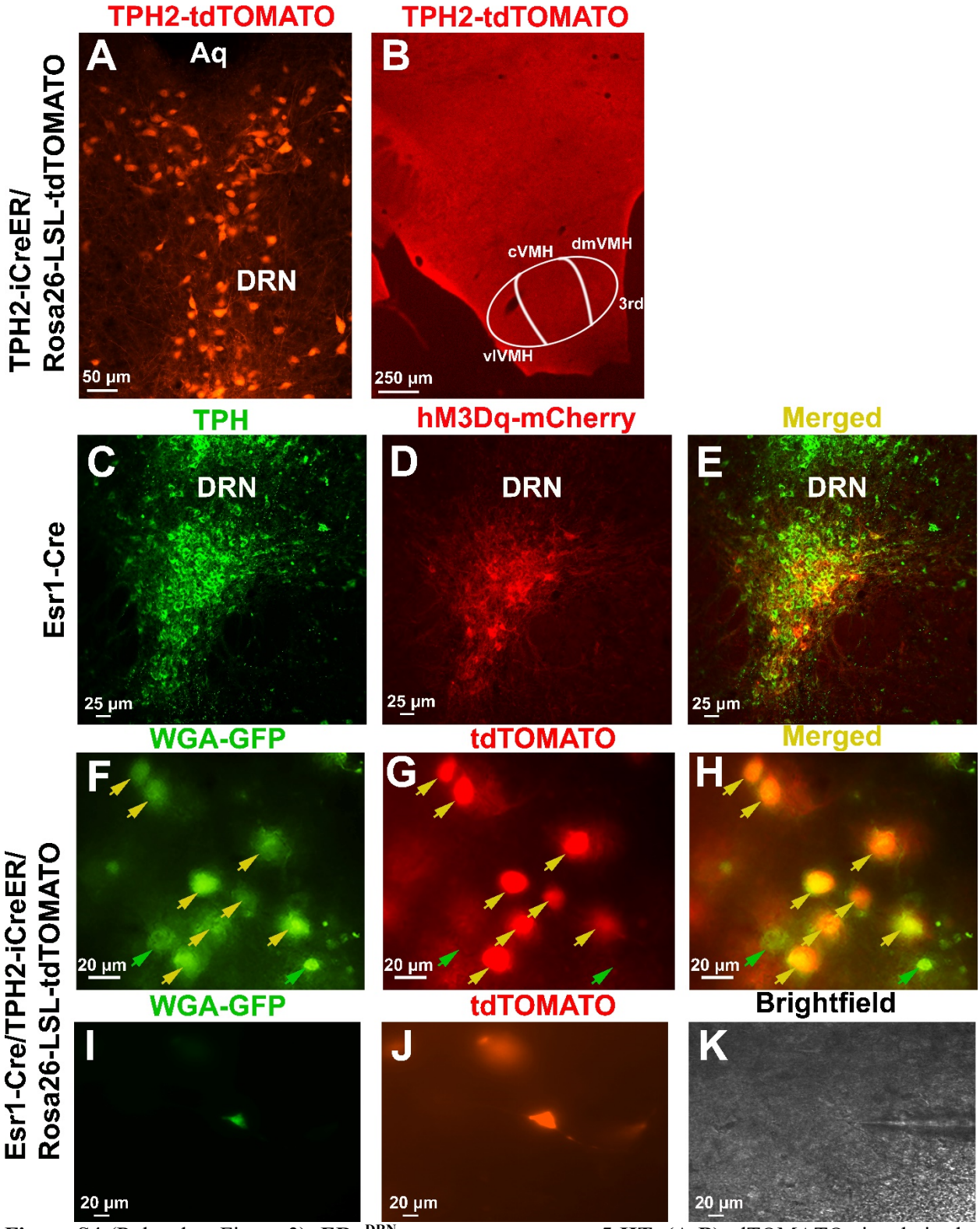

Figure S4 (Related to Figure 3). **ERα^{DRN} neurons co-express 5-HT.** **(A-B)** tdTOMATO signals in the DRN (A) and vlVMH (B) of female TPH2-iCreER/tdTOMATO mouse i.p. injected with tamoxifen (0.2 mg/g body weight). **(C-E)** Immunofluorescence staining of TPH (C), hM3Dq-mCherry (D), and merger (E) in the DRN of female Esr1-Cre mice injected with AAV-DIO-hM3Dq-mCherry virus into the DRN.

(F-H) Fluorescent signals of WGA-GFP (F), tdTOAMTO (G), and merger (H) in the DRN. Yellow arrows point to tdTOMATO(+)WGA-GFP(+) neurons while green arrows point to tdTOMATO(-)WGA-GFP(+) neurons. Female Esr1-Cre/TPH2-iCreER/Rosa26-LSL-tdTOMATO mice were injected with AAV2-DIO-ChR2-EYFP and anterograde transsynaptic tracer, Ad-iN/WED viruses, into the vlVMH. **(I-K)** Micrographic images showing a recorded yellow tdTOMATO(+)WGA-GFP(+) neuron that receives projection from $ER\alpha^{vlVMH}$ neurons in female mice. (I) the neuron patch clamped by a micropipette visualized under the green fluorescent microscope; (J): the same neuron visualized under red fluorescence microscope; (K): the same neuron visualized under brightfield microscope. Scale bar = 20 μm.

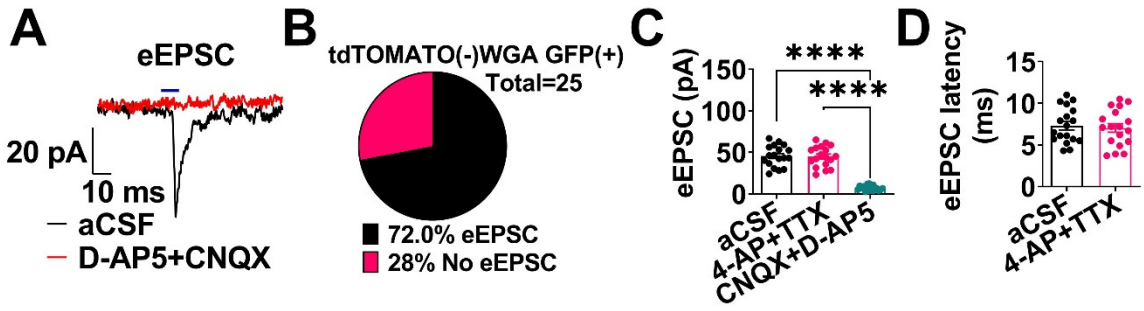

Figure S5 (Related to Figure 3). **ERα^{vlVMH}→DRN neural circuit stimulates 5-HT(-)^{DRN} neurons through glutamatergic neurotransmission.** **(A)** Representative eEPSC trace by blue light photostimulation (10 ms, 3 mW stimulation) after pre-incubation of aCSF or presynaptic inhibitors 30 μM CNQX+30 μM AP-5 in green tdTOMATO(-)WGA-GFP(+) neurons in the DRN. **(B)** Summary of 25 green tdTOMATO(-)WGA-GFP(+)in the DRN based on eEPSC response. **(C)** Summary of eEPSC amplitude after blue light photostimulation in the presence of aCSF, 1 μM 4-AP+1 μM TTX, or CNQX+D-AP5 (n = 18). **(D)** Summary of eEPSC latency after blue light photostimulation in the presence of aCSF or 4-AP+TTX (n = 18). (C) Results are presented as mean ± SEM. ****, $P < 0.0001$ in repeated-measures ANOVA analysis followed by post hoc Dunnett tests.

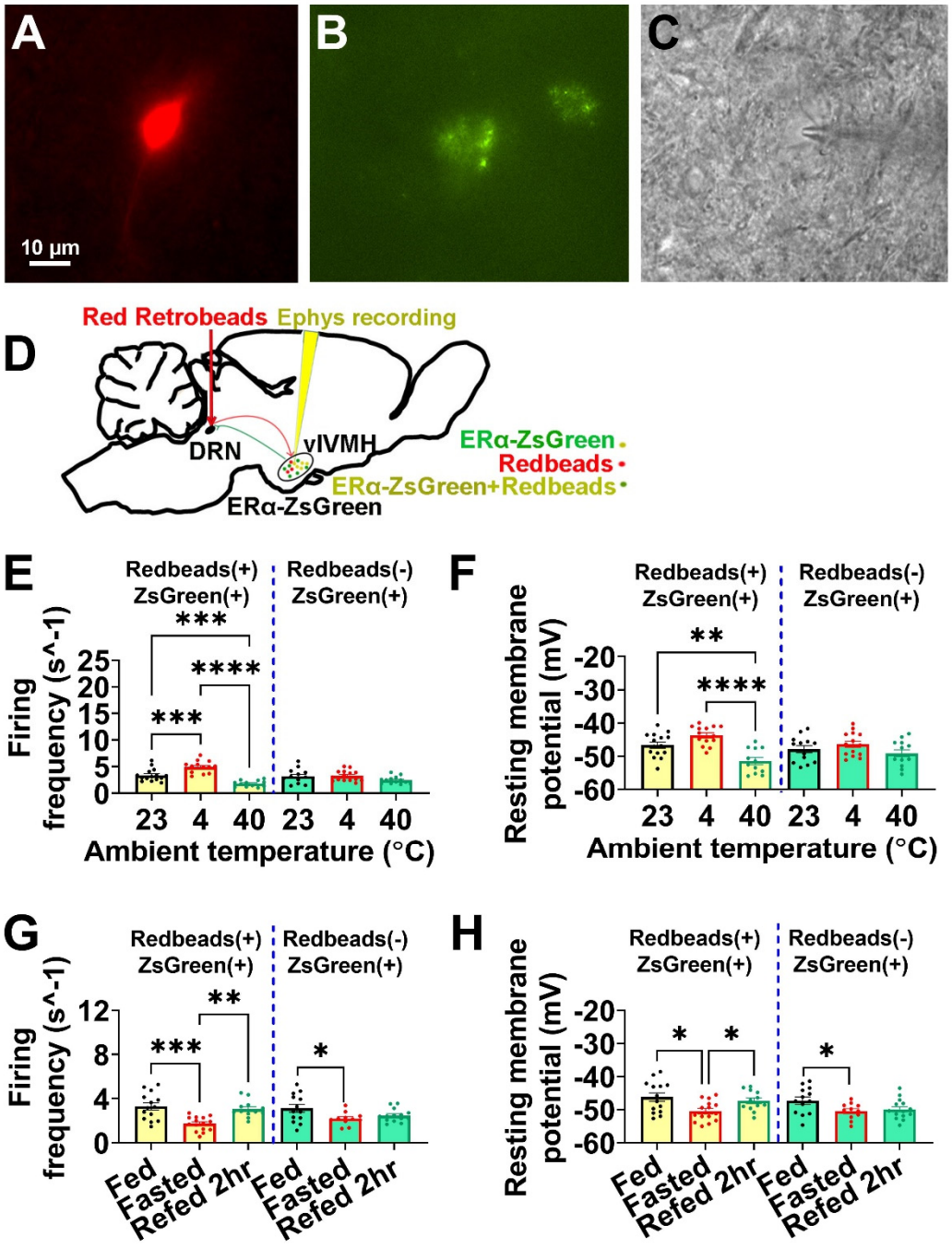

Figure S6 (Related to Figure 4). **Neural dynamics of DRN-projecting vs. non-DRN-projecting ERα^{vlVMH} neurons.** **(A-C)** Micrographic images showing a recorded DRN-projecting ERα^{vlVMH} neurons labeled with tdTOMATO(+)ZsGreen(+) dual yellow fluorescent colors in female mice. (A) Left panel: the neuron visualized under the red fluorescence microscope; (B) middle panel: the same neuron visualized under green fluorescence microscope; (C) right panel: the same neuron patch clamped by a micropipette visualized under the brightfield microscope. Scale bar = 10 μm. **(D)** Schematic of the experimental strategy using the Red Retrobeads to label and record the electrophysiological response of DRN-projecting and non-DRN-projecting ERα^{vlVMH} neurons in female ERα-ZsGreen mice. **(E-F)** Summary of firing frequency (D)

and resting membrane potential (E) when DRN-projecting ERα^{vlVMH} Redbeads(+)ZsGreen(+) or non-DRN-projecting ERα^{vlVMH} Redbeads(-)ZsGreen(+) neurons exposed to different temperatures (n = 15, 14, 12, 13, 15 or 13). **(G-H)** Summary data of firing frequency (F) and resting membrane potential (G) in different metabolic conditions (n = 14, 15, 12, 13, 11 or 14). (D-E and F-G) Results are presented as mean ± SEM. *, $P < 0.05$, **, $P < 0.01$, ***, $P < 0.001$,****, $P < 0.0001$ in one way ANOVA analysis followed by post hoc Tukey's tests.

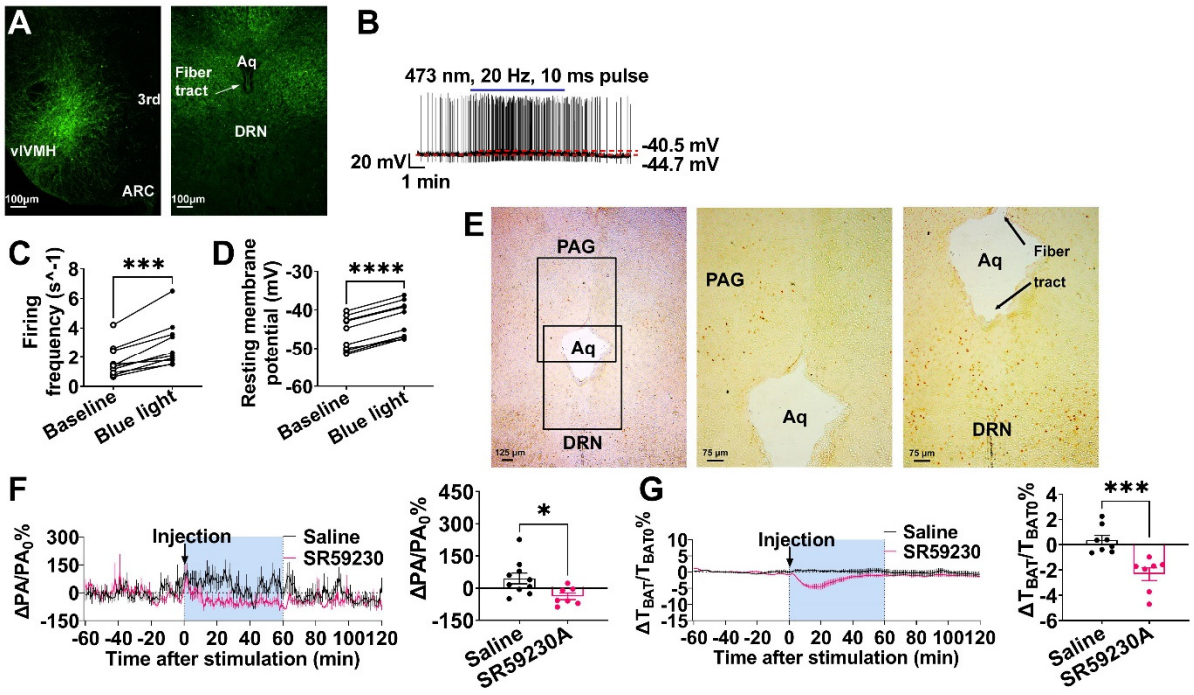

Figure S7 (Related to Figure 5). **Validation of ERα^{vlVMH}→DRN circuit activation.** **(A)** Immunofluorescence of EYFP in the vlVMH and DRN of female Esr1-Cre mice with AAV-DIO-ChR2-EYFP injected into the vlVMH and light fiber implanted into the DRN. **(B)** The electrophysiological responses of vlVMH EYFP-positive yellow neurons to blue light photostimulation in the vlVMH (20 Hz, 10 ms/pulse, 3 mW constant stimulation for 6 minutes) in female mice. **(C-D)** Summary of firing frequency (C) and resting membrane potential (D) before and after blue light stimulation (n = 10). **(E)** Post-hoc staining of cFOS on the DRN and the periaqueductal grey (PAG) samples after yellow/blue light photostimulation in the DRN (20 Hz, 10ms pulses, 3 mW constant stimulation for 5 minutes). **(F)** Effects of saline or SR59230 (0.5 mg/kg) i.p. injection on physical activity change (PA_0 represents average physical activity 1 hour before injection, ΔPA represents physical activity recording – PA_0) during 3-hrs recording (left panel) and average of physical activity change during 1 hour after i.p. injections (right panel). (n= 10 and 7). Female Esr1-Cre mice were injected with AAV-DIO-ChR2-EYFP virus into the vlVMH. Mice were given 1-hr yellow light stimulation (589 nm, 10 ms/pulse, 20 Hz, 3 s on and 2 s off for 1 h) right after the i.p. injections. **(G)** Effects of saline or SR59230 i.p. injection on BAT temperature change (T_{BAT0} represents average BAT temperature 1 hour before injection, ΔT_{BAT} represents BAT temperature recording – T_{BAT0}) during 3-hrs recording (left panel) and average of BAT temperature change during 1 hour after i.p. injections (right panel). (n= 10 and 7). (C-D) Data are presented for each cell. ***, $P < 0.001$, ****, $P < 0.0001$ in paired t-tests. (E-F) Results are shown as mean ± SEM. *, $P < 0.05$, ***, $P < 0.001$ in unpaired t-tests.

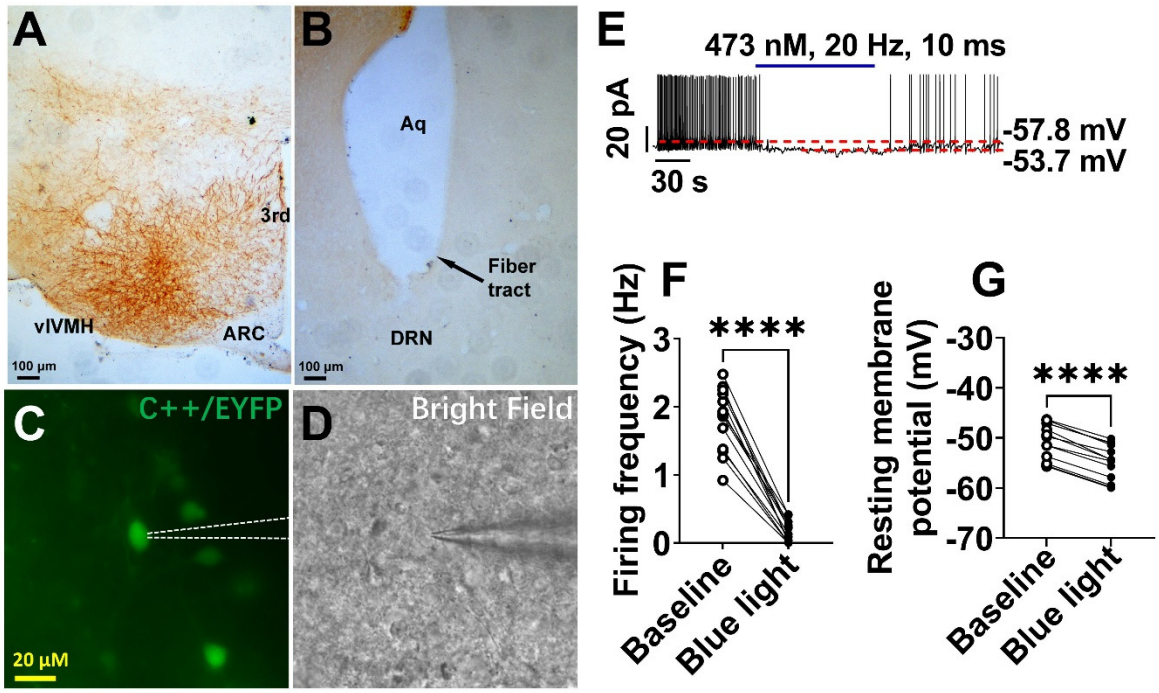

Figure S8 (Related to Figure 5). **Validation of ERα^{vlVMH}→DRN circuit inhibition.** **(A-B)** Immunohistochemistry staining of EYFP in the vlVMH (A) and DRN (B) of female Esr1-Cre mice with AAV-DIO-iC++-EYFP injected into the vlVMH and light fiber implanted into the DRN. **(C-D)** Micrographic images showing a recorded C++/EYFP (+) neurons in the vlVMH of female Esr1-Cre mice. Left panel (C): the neuron visualized under the green fluorescence microscope; right panel (D): the same neuron patch clamped by a micropipette visualized under the brightfield microscope. Scale bar = 20 µm. **(E)** The electrophysiological responses of vlVMH EYFP-positive neurons to blue light photostimulation in the vlVMH (20 Hz, 10 ms/pulse, 3 mW constant stimulation for 3 minutes). **(F-G)** Summary of firing frequency (F) and resting membrane potential (G) before and after blue light stimulation (n = 13). (F-G) Data are presented for each cell. ****, $P < 0.0001$ in paired t-tests.

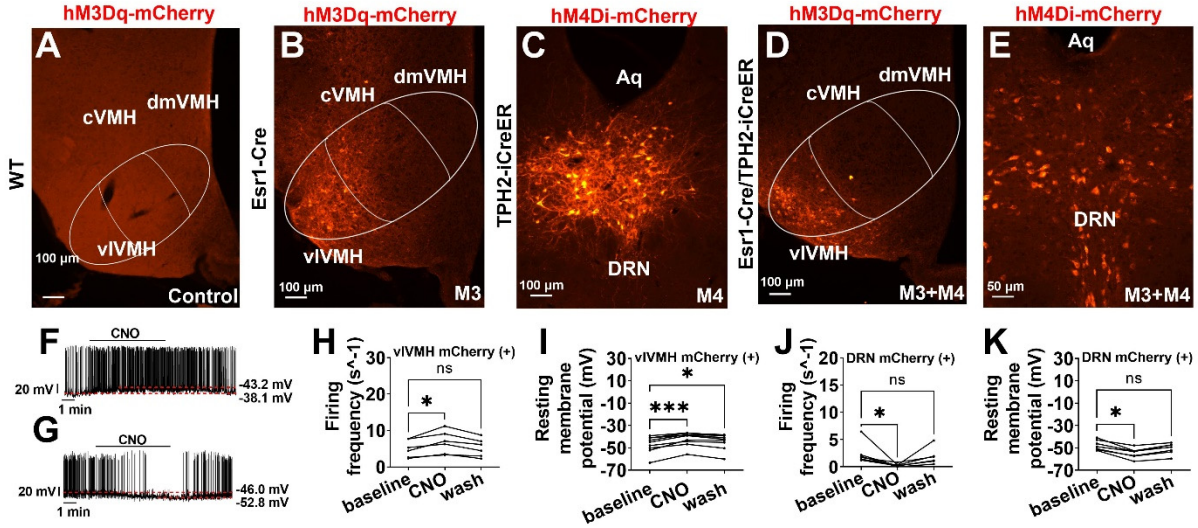

Figure S9 (Related to Figure 6). **Validation of ERα^{vlVMH} activation and of 5-HT^{DRN} inhibition by dual DREADD**. **(A-E)** Fluorescence of mCherry in the vlVMH of female WT mice injected with AAV-DIO-hM3Dq-mCherry virus into the vlVMH (A, Control), the vlVMH of female Esr1-Cre mice injected with AAV-DIO-hM3Dq-mCherry virus into the vlVMH (B, M3), the DRN of female TPH2-iCreER mice injected with AAV-DIO-hM4Di-mCherry virus into the DRN (C, M4), or the vlVMH and DRN of female Esr1-Cre/TPH2-iCreER mice injected with AAV-DIO-hM3Dq-mCherry virus into the vlVMH and AAV-DIO-hM4Di-mCherry virus into the DRN (D-E, M3+M4). **(F-G)** Representative traces of mCherry (+) cells in the vlVMH (F) and DRN (G) of female M3 + M4 mice before and after CNO treatment (5 µM). **(H-I)** Summary of firing frequency (H, n = 6) and resting membrane potential (I, n = 9) in mCherry (+) cells in the vlVMH before and after CNO treatment. **(J-K)** Summary of firing frequency (J, n = 6) and resting membrane potential (K, n = 7) in mCherry (+) cells in the DRN before and after CNO treatment. (H-K) Data are presented for each cell. *, $P < 0.05$, ***, $P < 0.001$ in repeated-measures ANOVA analysis followed by post hoc Dunnett tests.

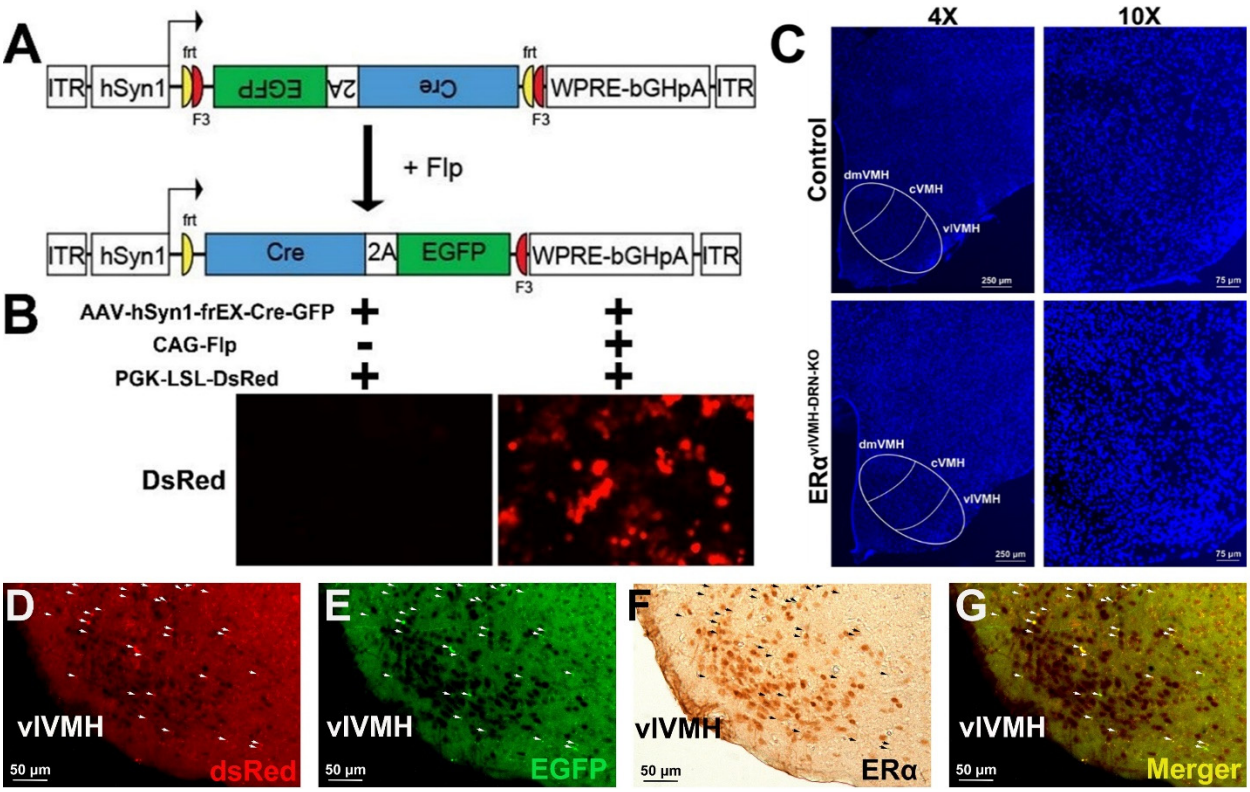

Figure S10 (Related to Figure 7). **Retrograde deletion of ERα.** **(A)** Schematic representation of Cre-EGFP-expressing AAV construct employing the fDIO (double frted inverse orientation) systems (AAV-hSyn1-frEX-Cre-GFP). ITR; inverted terminal repeats. hSyn1; human synapsin promoter 1. WPRE; woodchuck post-transcriptional regulatory element. bGHpA; bovine growth hormone poly(A) sequence. **(B)** Fluorescence of DsRed in HEK293 cells transfected with AAV-hSyn1-frEX-Cre-GFP + PGK-LSL-DsRed, or AAV-hSyn1-frEX-Cre-GFP + PGK-LSL-DsRed + CAG-Flpe. **(C)** DAPI staining in the vlVMH of female control and ERα$^{vlVMH\text{-}DRN\text{-}KO}$ mice. **(D-G)** Expression of dsRed (D), EGFP (E), ERα (F), and merger (dsRed+EGFP, G) in the vlVMH of ERα$^{vlVMH\text{-}DRN\text{-}KO}$ mice.

KEY RESOURCES TABLE

REAGENT or RESOURCE	SOURCE	IDENTIFIER
Antibodies		
Anti-Wheat germ agglutinin antibody	Vector Laboratories	Cat# AS2024, RRID:AB_2315609
Donkey anti-Goat IgG (H+L) Cross-Adsorbed Secondary Antibody, Alexa Fluor 488	Thermo Fisher Scientific	Cat# A-11055, RRID:AB_2534102
5-HT (Serotonin) Rabbit Antibody	ImmunoStar	Cat# 20080, RRID:AB_572263
Goat anti-Rabbit IgG (H+L) Highly Cross-Adsorbed Secondary Antibody, Alexa Fluor 594	Thermo Fisher Scientific	Cat# A-11037, RRID:AB_2534095
Living Colors® DsRed Polyclonal Antibody	Takara Bio	Cat# 632496, RRID:AB_10013483
Biotin-SP-AffiniPure Fab Fragment Donkey Anti-Rabbit IgG (H+L) antibody	Jackson ImmunoResearch Labs	Cat# 711-067-003, RRID:AB_2340595
VECTASTAIN Elite ABC-Peroxidase Kit	Vector Laboratories	Cat# PK-6100, RRID:AB_2336819
Anti-Estrogen Receptor alpha antibody	Millipore	Cat# 06-935, RRID:AB_310305
Green Fluorescent Protein (GFP) Antibody	Aves Labs	Cat# GFP-1020, RRID:AB_10000240
cFos (9F6) Rabbit mAb antibody	Cell Signaling Technology	Cat# 2250, RRID:AB_2247211
DsRed (E-8) Alexa Fluor 594	Santa Cruz Biotechnology	Cat# sc-390909, RRID:AB_2801575
Sheep Anti-Tryptophan Hydroxylase Polyclonal antibody, Unconjugated	Millipore	Cat# AB1541, RRID:AB_90754
Bacterial and Virus Strains		
pAAV-hSyn-DIO-hM3D(Gq)-mCherry	The Vector Core at the University of North Carolina at Chapel Hill	RRID:Addgene_44361
pAAV-hSyn-DIO-hM4D(Gi)-mCherry	The Vector Core at the University of North Carolina at Chapel Hill	RRID:Addgene_44362
pAAV-EF1a-DIO-hChR2(H134R)-P2A-EYFP	The Vector Core at the University of North Carolina at Chapel Hill	RRID:Addgene_139283
pAAV-EF1a-DIO iC++-eYFP	The Vector Core at the University of North Carolina at Chapel Hill	N/A
CAV2-Cre	Montpellier vector platform	N/A
Ad-iN/WED	Martin Myers	N/A
AAV2-EF1a-FLEX-GT	Viral Vector Core - Salk Institute for Biological Studies	RRID:Addgene_26198
AAV2-EF1a-FLEX-GTB	Viral Vector Core - Salk Institute for Biological Studies	RRID:Addgene_26197
EnVA-G-deleted Rabies-mCherry	Viral Vector Core - Salk Institute for Biological Studies	N/A

ΔG Rabies FLPo-dsRedXpress	Viral Vector Core - Salk Institute for Biological Studies	N/A
AAV-hSyn1-frEX-Cre-GFP	Yong Xu	N/A
AAV2-CMV-GFP	The Vector Core at the University of North Carolina at Chapel Hill	RRID:Addgene_49055
Chemicals, Peptides, and Recombinant Proteins		
CNQX	Tocris.inc	Cat# 0190
17β-Estradiol	MedChem Express	Cat# HY-B0141
Clozapine N-oxide	MedChem Express	Cat# HY-17366
SR59230A	Millipore&Sigma	Cat# S8688
tetrodotoxin	R&D system	Cat# 1078
(+)-Bicuculline	Tocris.inc	Cat# 0130
D-AP5	Tocris.inc	Cat# 0106
Red Retrobeads	Lumafluor.inc	Red Retrobeads™ IX
Experimental Models: Organisms/Strains		
Mouse: Rosa26-LSL-tdTOMATO: B6.Cg-Gt(ROSA)26Sor$^{tm14(CAG-tdTomato)Hze}$/J	Jackson Laboratory	Cat# 007914, RRID:IMSR_JAX:007914
Mouse: Esr1$^{lox/lox}$: ERαfl/fl	Sohaib A. Khan	N/A
Mouse: ERα-ZsGreen	Yong Xu	N/A
Mouse: Esr1-Cre: B6N.129S6(Cg)-Esr1tm1.1(cre)And/J	Jackson Laboratory	Cat# 017911, RRID:IMSR_JAX:017911
Mouse: TPH2-iCreER: STOCK Tg(Tph2-icre/ERT2)6Gloss/J	Jackson Laboratory	Cat# 016584, RRID:IMSR_JAX:016584
Recombinant DNA		
Cre Shine	Addgene	RRID:Addgene_37404
pCAG-Flpe	Addgene	RRID:Addgene_13787
Software and Algorithms		
pClamp 10.3 software	Molecular Devices	N/A
Vitalview® Telemetry software	STARR Life Sciences	N/A
GraphPad Prsim 9	GraphPad	N/A